Proceedings of the Eleventh EGS4 Users' Meeting in Japan, KEK Proceedings 2003-15, p.88-96

POINT SPREAD FUNCTION OF WATER SLAB AND METAL PLATE IN PORTAL IMAGING

S. Miyajima, S. Yamada and K. Murase
Graduate School of Medicine, Course of Health Sciences, Osaka University
1-7 Yamadaoka, Suita, Osaka, 565-0871, Japan
E-mail: satoshi@sahs.med.osaka-u.ac.jp

Abstract

The point spread functions (PSFs), which show the spread of signal in water slabs and metal plates (Al, Cu and W), were calculated with the Monte Carlo method. The parameters were the energy of monoenergetic incident photons (1 $\sim$ 20 MeV), the slab thicknesses (10-30 cm for water slabs and 0.5-5 mm for metal plates), and the air gaps in case of water slabs (0-100 cm). The scatter-to-primary ratios of water slabs and the conversion factors of metal plates are calculated using the calculated results.

1 Introduction

Accurate dose delivery to tumor volume with sparing the surrounding healthy tissues is essential for radiation therapy. The portal image is the image which is made using the x-ray beam that exits from a patient during radiotherapy. The relation between the irradiated volume and the anatomical structure (i.e. bone or air in the body) of a patient is shown to identify patient positioning errors in the 'double exposure' portal image. The image is obtained superimposing the image with a shaped collimator on that with a collimator wide open. Since the energy of x-rays used in radiotherapy is relatively high compared to that used in diagnostic radiology, the portal image suffers from low contrast and may lack details of the anatomic structure to determine if the prescribed volume is irradiated. [1]

The principle of the portal imaging is in Figure 1. X-rays from a source irradiate an object and an x-ray image with transmitted x-rays is formed below the object. The x-ray image is converted to an electron image in metal plates mainly by the Compton scattering. The metal plate also rejects secondary x-rays, electrons and positrons from the object by absorption. A phosphor screen is often used to convert the electron image to an optical photon image. The electron or optical photon image are detected by a sensor. The sensors used in the portal imaging are the film systems and the electronic portal imaging devices (EPIDs). The EPIDs include the devices such as liquid matrix ionization chambers, video-camera systems and flat-panel imaging systems.[1]-[4]

The portal image with MeV x-rays reflects the variation of density in the body because the Compton scattering is dominant in this energy range [Fig. 2(a)]. [2] The differences in the attenuation coefficients of various tissues in the body are small in the MeV energy range [Fig. 2(b)]. As a result, the image contrast in the portal image is small.

In transmission radiography, the x-rays reaching the detector consist of primary (unscattered) and scattered components. While the primary components contribute to the signal in the resultant image, the scatter components may reduce image contrast and introduce noise. The differences in the transmission of primary x-rays in different tissues are the source of image contrast. As the

[1]While MeV x-rays ($\sim$ 20 MeV) are used in portal imaging, keV x-rays ($\sim$ 150 keV) are utilized in diagnostic radiology.

[2]The probability of the Compton scattering is nearly dependent on the density of materials. The diagnostic x-ray image reflects not only the variation of density but that of the atomic number. See Figure 2(b) for reference.

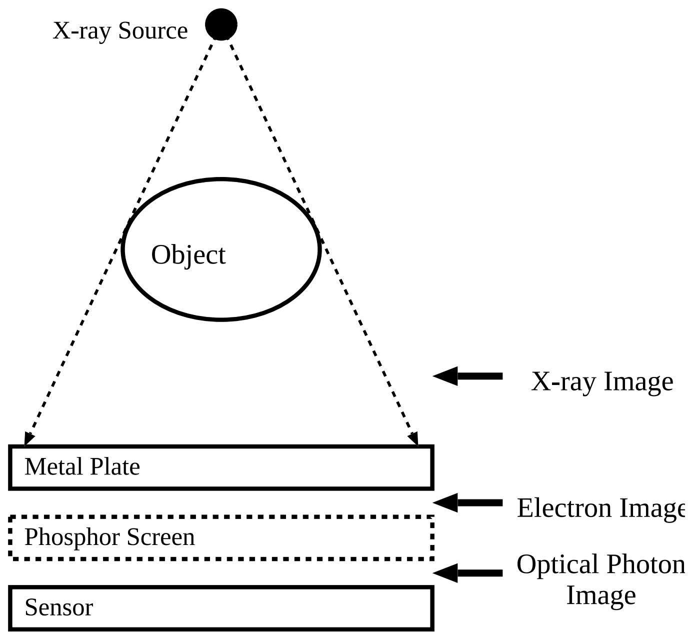

Figure 1: The principle of the portal imaging. The x-ray image by transmitted x-rays is converted to an electron image in metal plates. The electron image (or an optical photon image which is generated with a phosphor screen) is detected by a sensor.

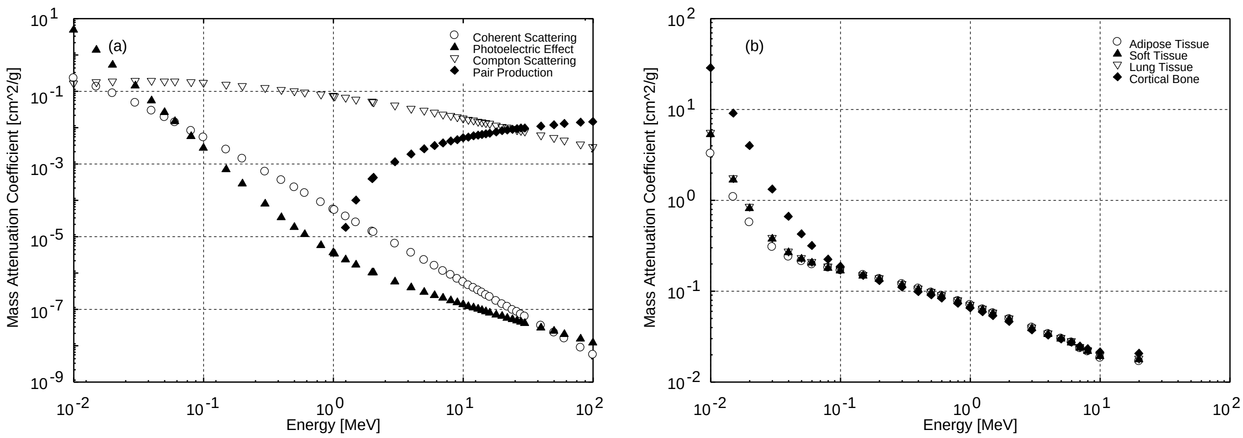

Figure 2: (a) The dependence of the mass attenuation coefficients of each interaction in water on x-ray energy. Note that the Compton scattering predominates in the MeV energy range. (b) The dependence of the mass attenuation coefficients of various tissues in the body on x-ray energy. It should be noted that the coefficients are dependent only on density in the MeV energy range.

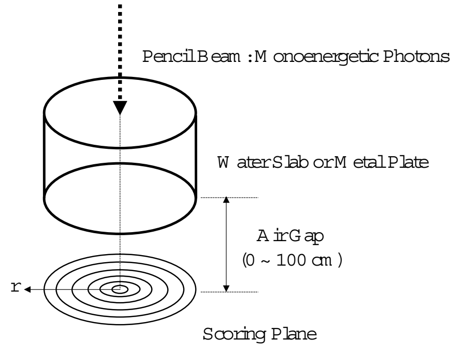

Figure 3: Model in the calculation of the point spread functions. The parameters in the calculation were (i) photon energy [1 $\sim$ 20 MeV], (ii) slab thicknesses [10 $\sim$ 30 cm for water slabs and 0.5 $\sim$ 5 mm for metal plates], (iii) the air gaps in case of water slabs [0 $\sim$ 100 cm], and (iv) the kinds of metal plates [Al, Cu and W].

differences are small in the megavoltage energy range, the portal image is very susceptible to noise and the quality of the portal image is poorer than that of the diagnostic x-ray image.

The signal in the portal image is based on the primary transmitted x-rays: the difference in the intensity of them forms the subject contrast. The signal is spread by secondary particles during the transmission in the object and the conversion of x-rays to electrons in metal plates (and that of electrons to optical photons in a phosphor screen). These phenomena affect the signal transfer and result in the blurring of image. The signal spread attributed to the x-ray source and the detector response also contributes to the blurring.[4]-[6]

The point spread functions of water slabs and metal plates were calculated with the Monte Carlo method. Water slabs and metal plates are chosen because they are indispensable for the portal imaging. The spread of photons, electrons and positrons emitted from the bottom of water slabs and metal plates was estimated. The effects of x-ray energy, water or metal thickness, and the kind of metals on the signal spread are shown. The scatter-to-primary ratios (SPRs) of water slabs and the conversion factors of various metal plates are also calculated.

2 Materials and Methods

The point spread functions (PSFs) of water slabs and metal plates were calculated with the Monte Carlo method. The model in the calculation is in Fig. 3. A pencil beam of monoenergetic photons was incident on the cylindrical slab of water or metal. The energy of incident photons was from 1 to 20 MeV. The metal plates of aluminum, copper and tungsten were incorporated in the calculation. The diameter of the cylinder was 30 cm ϕ. The thickness of water slabs and metal plates was 10, 20 and 30 cm and 0.5, 1, 3 and 5 mm, respectively. The energy fluence of particles (i.e. photons, electrons and positrons) emitted from the bottom of the water slabs or metal plates was registered at the scoring plane as a function of the distance from the center r. The PSFs were normalized to the area of each scoring region, and to the energy fluence of incident photons. In case of water slabs, the air gap (0, 50 and 100 cm) was set below the slabs to estimate the effect on the scatter rejection.

The scatter-to-primary ratios (SPRs), which are the ratios of the scatter components to the primary components in transmitted beams, of water slabs are calculated: the smaller the SPR is, the less the fraction of scatter is in the x-ray image. The conversion factors, which are the ratios of the energy fluence of electrons or positrons to that of incident photons, of metal plates are also calculated.

The EGS4 code was used in the calculation. The PRESTA option was utilized in the calculation. The photoelectric effect, the coherent scattering, the Compton scattering with free electrons, the pair production were included. The production of the bremsstrahlung photons was taken into account. Both of the cutoff energy of photons and electrons were 10 keV (i.e. PCUT = 0.01; and ECUT = 0.561;) in the calculation.

3 Results and Discussion

The examples of calculated results are shown in Figure 4 to 8. As the signals are transfered mainly by photons in water slabs and by electrons and positrons in metal plates, only the results for them are shown in this section.

3.1 Point spread function and scatter-to-primary ratio of water slabs

Figure 4 shows the point spread functions (PSFs) of 20 cm water with various air gaps. The relative energy fluence at 0 cm is mainly attributed to the primary photons: the rest is due to the scatter components. The scatter components are reduced substantially by the air gaps. The effect of incident photon energy on the PSFs is apparent in the air gap of 0 cm. The effect is supposed to be mainly due to the dependence of the scattering angle on photon energy in the Compton scattering. The dependence is far less in the larger air gaps. The same tendency is observed with water slabs of 10 cm and 30 cm.

The scatter-to-primary ratios (SPRs) of a 20 cm water slab are shown in Figure 5. The SPRs are dependent on photon energy: the fraction of scatter in transmitted beams is smaller with incident photons of higher-energy. The SPRs are also smaller with the larger air gaps. The SPRs also depend on water thickness: they are larger with thicker water slabs.

3.2 Point spread function and conversion factor of metal plates

The PSFs of electron and positron in copper plates are shown in Figure 6. The spread of electrons and positrons is dependent on photon energy. The spread is larger with thicker metals. Though the same tendency was observed with Al and W plates, the dependence of the spread on photon energy is small in tungsten plates (Fig. 7).

The conversion factors of electrons and positrons of metal plates are shown in Figure 8. The conversion factors depend on photon energy. The factors are also dependent on metal thickness especially in aluminum. In tungsten, however, the dependence is minimal because the generation of electron and positron is almost saturated in a tungsten plate of 0.5 mm thickness.

3.3 Advantage of Monte Carlo calculation over experimental study

The advantage of the Monte Carlo (MC) calculation over the experimental study in image analysis is that the effects of various parameters on image quality are estimated separately. Therefore, the limiting factor of image quality can be found and the optimization of the imaging system is possible with the results of the MC calculation.

4 Conclusions

The point spread functions of water slabs (10-30 cm thickness) and metal plates (Al, Cu and W, 0.5-5 mm thickness) were calculated with the EGS4 code. The photon spread in water slabs and

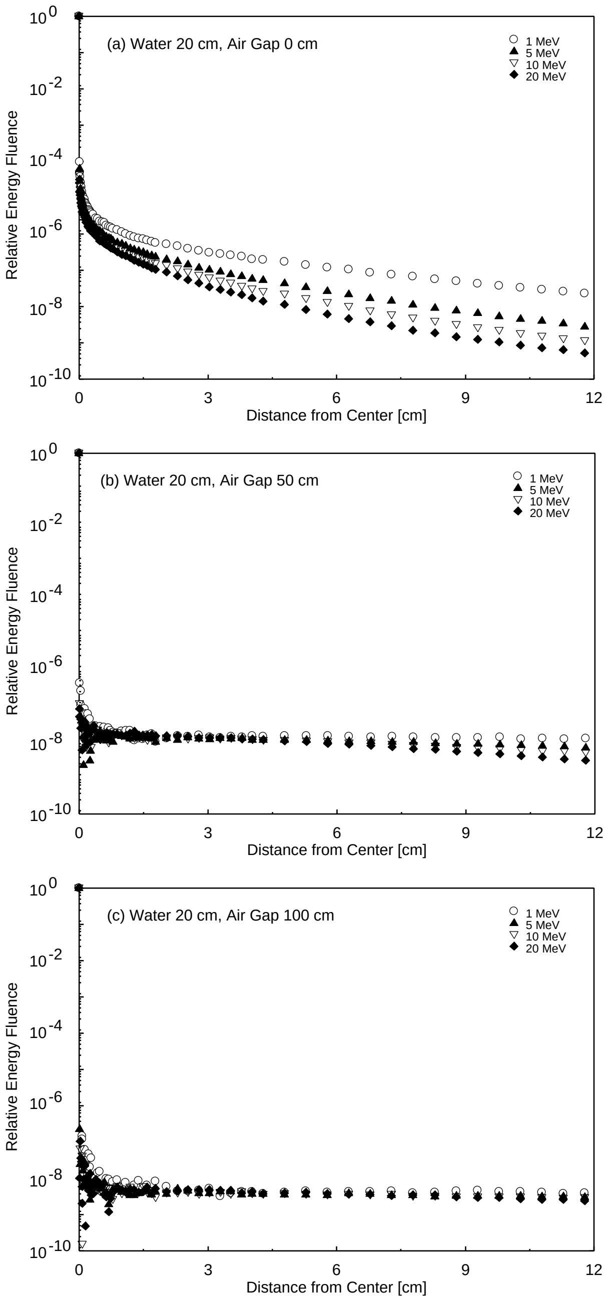

Figure 4: The point spread functions of the water slab of 20 cm thickness with the different air gaps. The parameters were photon energy.

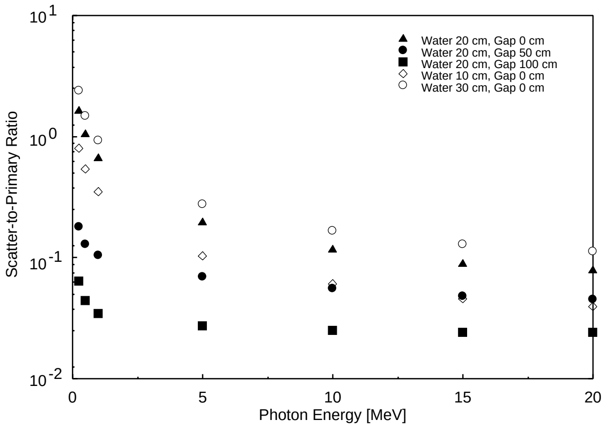

Figure 5: The scatter-to-primary ratios of water slabs with different air gaps. Those of water slabs of different thicknesses were also shown.

the electron or positron spread in metal plates are shown in this paper. The scatter-to-primary ratios (SPRs) of water and the conversion factors of metal plates are also shown. The Monte Carlo calculation is useful because the effects of each parameter on the portal imaging can be assessed separately. The results contribute to the optimization of the portal imaging system.

Acknowledgments

This work was partially supported by Grant-in-Aid for JSPS Fellows No. 15-03727 from the ministry of education, culture, sports, science, and technology of Japan.

References

[1] A. L. Boyer, L. Antonuk, A. Fenster, M. V. Herk, H. Meertens, P. Munro, L. E. Reinstein and J. Wong, *"A review of electronic portal imaging devices (EPIDs),"*, Med. Phys., 19, 1-16 (1992).

[2] L. E. Antonuk, *"Electronic portal imaging devices: a review and historical perspective of contemporary technologies and research,"* Phys. Med. Biol., 47, R31-R65 (2002).

[3] K. A. Langmack, *"Portal imaging,"* Brit. J. Radiol., 74, 789-804 (2001).

[4] M. G. Herman, J. M. Balter, D. A. Jaffray, K. P. McGee, P. Munro, S. Shalev, M. V. Herk and J. W. Wong, *"Clinical use of electronic portal imaging: report of AAPM radiation therapy committee task group 58,"* Med. Phys., 28, 712-737 (2001).

[5] P. Munro, J. A. Rawlinson and A. Fenster, *"Therapy imaging: source sizes of radiotherapy beams,"* Med. Phys., 15, 517-524 (1988).

[6] D. A. Jaffray, J. J. Battista, A. Fenster and P. Munro, *"X-ray sources of medical linear accelerators: focal and extra-focal radiation,"* Med. Phys., 20, 1417-1427 (1993).

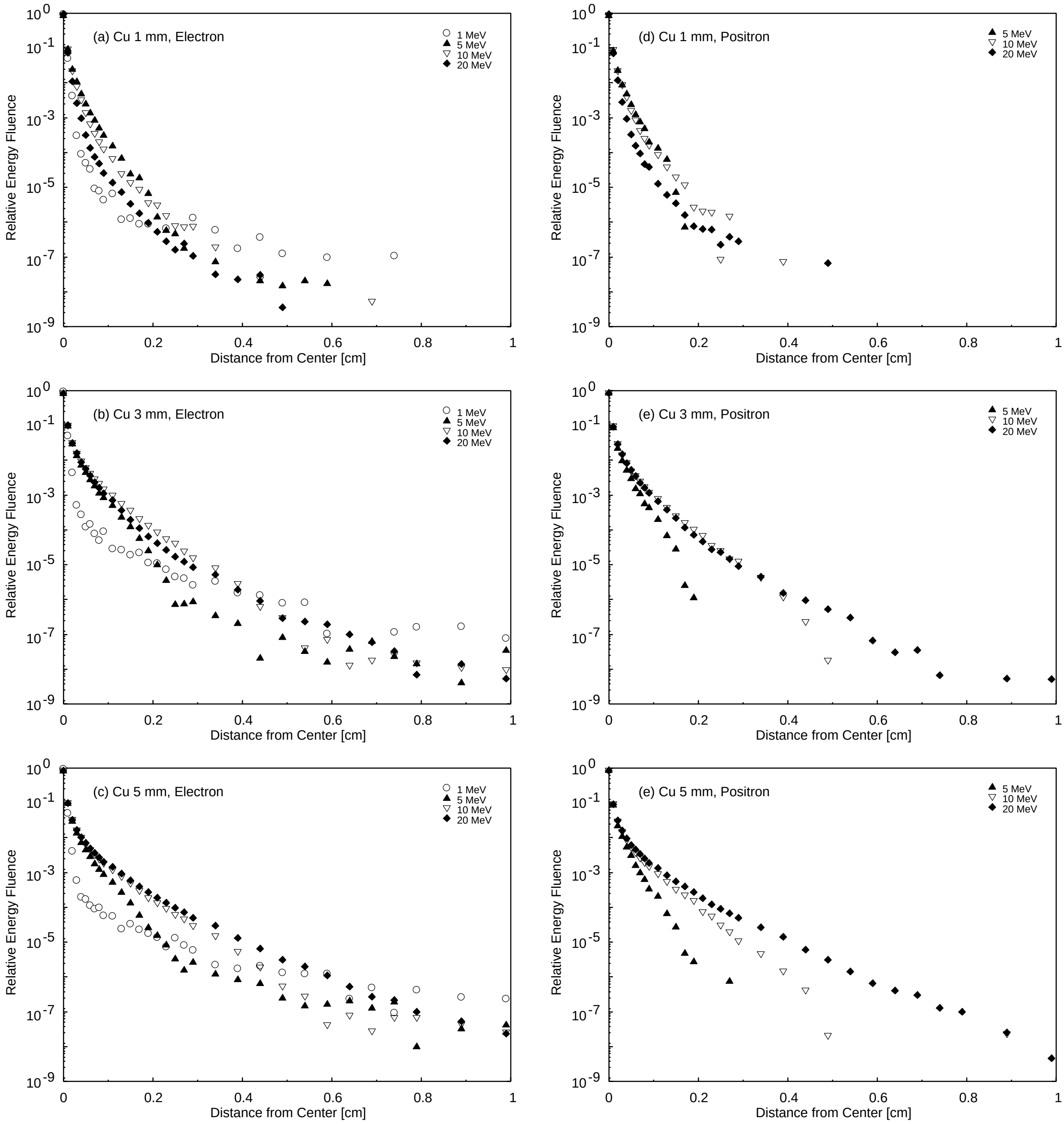

Figure 6: The point spread functions of copper plates of electrons [(a) ∼ (c)] and positrons [(d) ∼ (f)]. The parameters were incident photon energy.

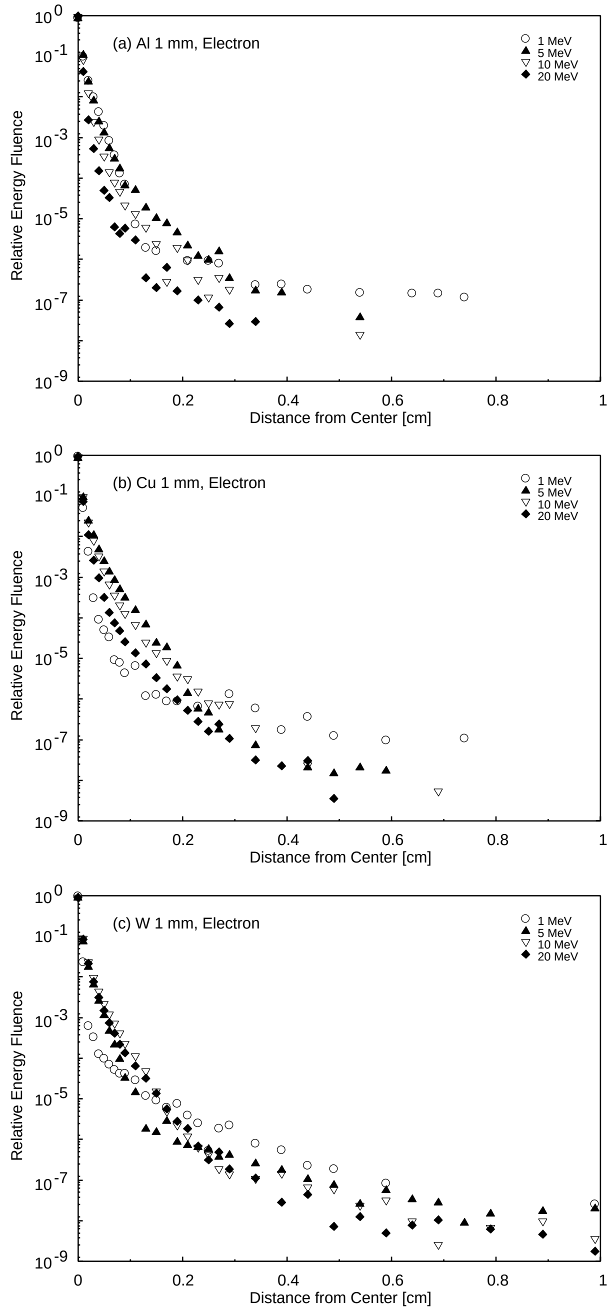

Figure 7: The point spread functions of electrons of various metal plates. The parameters were incident photon energy.

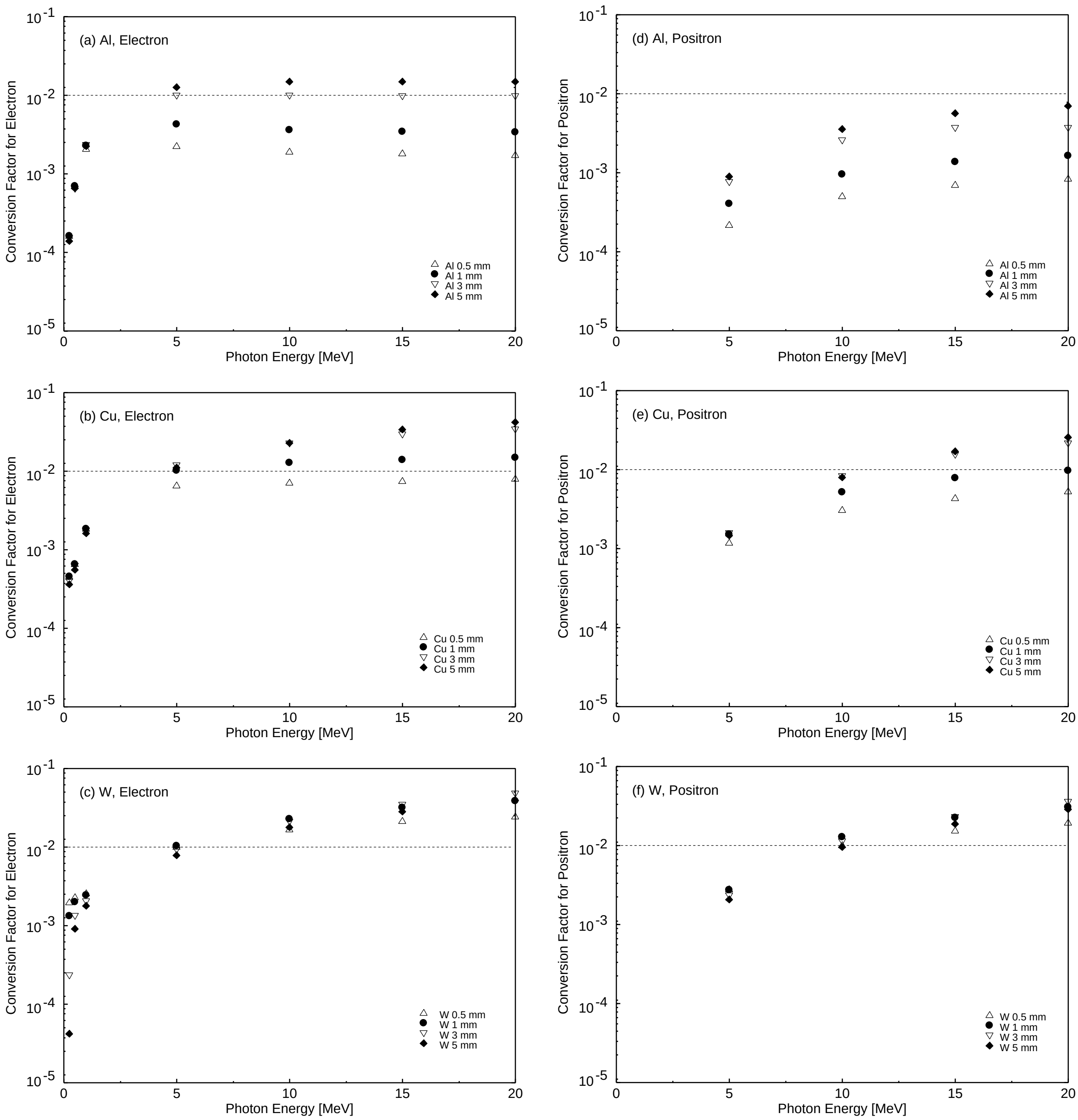

Figure 8: The conversion factors of electrons [(a) $\sim$ (c)] and positrons [(d) $\sim$ (f)] in aluminum, copper and tungsten plates of different thicknesses. The parameters were thicknesses of metal plates. Note that the horizontal broken line in each figure indicates 1%.